Available online at www.sciencedirect.com
SCIENCE DIRECT®
Physics Letters B 636 (2006) 46–50
PHYSICS LETTERS B
www.elsevier.com/locate/physletb

Using dileptons to probe the color glass condensate

M.A. Betemps [a,b,*], M.B. Gay Ducati [a]

[a] *High Energy Physics Phenomenology Group, GFPAE, Instituto de Física, Universidade Federal do Rio Grande do Sul, Caixa Postal 15051, CEP 91501-970, Porto Alegre, RS, Brazil*

[b] *Conjunto Agrotécnico "Visconde da Graça", CAVG, Universidade Federal de Pelotas, Caixa Postal 460, CEP 96060-290, Pelotas, RS, Brazil*

Received 31 January 2006; accepted 8 March 2006

Available online 20 March 2006

Editor: M. Cvetič

Abstract

The rapidity and transverse momentum dependence of the nuclear modification ratio for dilepton production at RHIC and LHC is presented, calculated in the color glass condensate (CGC) framework. The transverse momentum ratio is compared for two distinct dilepton mass values and a suppression of the Cronin peak is verified even for large mass. The nuclear modification ratio suppression in the dilepton rapidity spectra, as obtained experimentally for hadrons at RHIC, is verified for LHC energies at large transverse momentum, although not present at RHIC energies. The ratio between LHC and RHIC nuclear modification ratios is evaluated in the CGC, showing the large saturation effects at LHC compared with the RHIC results. These results consolidate the dilepton as a most suitable observable to investigate the QCD high density approaches.

PACS: 11.15.Kc; 24.85.+p

1. Introduction

In the most recent data on hadrons transverse momentum spectra in high energy collisions, some interesting results have been pointed out [1,2]. The comparison between transverse momentum distribution in d–Au and p–p, and in central and peripheral collisions has being the main object of investigation. These comparisons are performed introducing the nuclear modification ratio,

$$R_{d\mathrm{Au}} = \frac{\frac{dN^{d\mathrm{Au}\to hX}}{dy\,dp_T^2}}{N_{\mathrm{coll}}\frac{dN^{pp\to hX}}{dy\,dp_T^2}}, \tag{1}$$

where the normalization factor N_{coll} is the number of binary collisions, y and p_T are the rapidity and transverse momentum of the hadrons, respectively. For the case of d–Au collisions at mid-rapidity $y \approx 0$, the ratio $R_{d\mathrm{Au}}$ becomes smaller than 1 at small p_T, larger than 1 at intermediated values of p_T and saturates at 1 for large p_T. This implies a peak at intermediate p_T (2–5 GeV), which is called Cronin effect or Cronin peak. At large rapidities a suppression of the ratio $R_{d\mathrm{Au}}$ was observed and a flat behavior at large p_T is found (disappearance of the Cronin peak). Another ratio should be evaluated, considering the same process, now taking a ratio between central and peripheral process in order to avoid systematic errors. In this case the ratio R_{CP} should be taken instead of the ratio $R_{d\mathrm{Au}}$. In both defined ratios, the observations are the same, a significant reduction of the yield of charged hadrons measured in d–Au collisions when compared with the p–p collisions at forward rapidities [2].

The main interest related to the Cronin effect in the literature is regarding the hadron p_T spectra, however, the dilepton production should also be considered as an observable to study this effect. The dileptons analyzed in the context of the color glass condensate (e.g., [8–11]) present the same features of the Cronin effect in such approach [12] and do not present final state interactions, providing more clear information on the color glass condensate. In this work, the ratio between p–Au and p–p differential cross section is evaluated, analyzing the transverse momentum distribution at a fixed rapidity and the

* Corresponding author.
E-mail addresses: marcos.betemps@ufrgs.br (M.A. Betemps), beatriz.gay@ufrgs.br (M.B. Gay Ducati).

0370-2693/$ – see front matter
doi:10.1016/j.physletb.2006.03.021

rapidity distribution of the dileptons for 6 GeV mass. A comparison between distinct dilepton mass results in the transverse momentum distribution at a fixed rapidity is performed.

The origin of the Cronin effect can be explained in different ways, depending on the rapidity region. In d–Au collisions and central rapidities, the Cronin peak is due to the multiple scattering of the deuterium constituents with the nuclear environment. At forward rapidities the suppression of the ratio could be a manifestation of the CGC [6,7] (or effect of $x_F \to 1$ [3]). At backward rapidities in d–Au collisions, the nuclear modification ratio should present different behavior once comparing with the hadron and dilepton p_T spectra [4]. Concerning dilepton at backward rapidities, this point is being under investigation in another work [5].

2. Dilepton production in the CGC approach

The dilepton production at high energies is dominated by the bremsstrahlung of a virtual photon by a quark from a hadron interacting with a dense background gluonic field of the nucleus, and afterwards decaying into a lepton pair. In order to do the required calculation one considers only the diagrams where the photon emission occurs before or after the interaction with the nucleus, since the emission considering both before and after the interaction is suppressed [13].

The dilepton production is investigated in the context of the color glass condensate, which is a QCD classical effective theory to deal with the high dense partonic system [14]. In this theory, the small x gluons are radiated from fast moving color sources, which are partons with larger values of x, being described by a color source density ρ_a with internal dynamics frozen by Lorentz time dilatation, thus forming a color glass. The observables are obtained by means of an average over all configurations of the color sources, performed through a weight functional $W_{\Lambda^+}[\rho]$, which depends upon the dynamics of the fast modes, and upon the intermediate scale Λ^+, which defines fast ($p^+ > \Lambda^+$) and soft ($p^+ < \Lambda^+$) modes. The effective theory is valid for soft momenta of order Λ^+. Indeed, reaching much softer scale, there are large radiative corrections which invalidate the classical approximation. The modifications to the effective classical theory are governed by a functional, nonlinear, evolution equation JIMWLK [15,16] for the statistical weight functional $W_{\Lambda^+}[\rho]$ associated with the random variable $\rho_a(x)$.

The hadronic cross section of the process is obtained employing the collinear factorization and considering the forward rapidity region [8,17],

$$\frac{d\sigma^{pA\to ql^+l^-X}}{dp_T^2\,dM\,dy} = \frac{4\pi^2}{M} R_A^2 \frac{\alpha_{\rm em}^2}{3\pi} \int \frac{dl_T}{(2\pi)^3} l_T \mathcal{W}(p_T, l_T, x_1) C(l_T, x_2, A), \quad (2)$$

with y being the rapidity, s represents the squared center of mass energy and l_T is the total transverse momentum transfer between the nucleus and the quark. R_A is the nuclear radius, M is the lepton pair mass, x_1 and x_2 are the momentum fractions carried by the quark from the proton and by the gluonic field from the nucleus, respectively, defined in the formal way. The expression (2) is restricted to the forward region only, which means positive rapidities y. The function $\mathcal{W}(p_T, l_T, x_1)$ can be written as [17]

$$\begin{aligned}\mathcal{W}(p_T, l_T, x_1) &= \int_{x_1}^{1} dz\, z F_2\big(x_1/z, M^2\big) \\ &\quad \times \left\{ \frac{(1+(1-z)^2) z^2 l_T^2}{[p_T^2 + M^2(1-z)][(p_T - z l_T)^2 + M^2(1-z)]} \right. \\ &\quad - z(1-z)M^2 \left[\frac{1}{[p_T^2 + M^2(1-z)]} \right. \\ &\quad \left. \left. - \frac{1}{[(p_T - z l_T)^2 + M^2(1-z)]} \right]^2 \right\}, \end{aligned} \quad (3)$$

which selects the values of l_T larger than p_T [8]. Here, $F_2(x_1/z, M^2)$ is the partonic structure function, which takes into account the quark distribution of the proton projectile and $z \equiv p^-/k^-$ (light-cone variables) is the energy fraction of the proton carried by the virtual photon. In Eq. (2) the function $C(l_T, x_2, A)$ is the field correlator function which, disregarding the energy and nuclear dependence, can be defined by [18],

$$C(l_T) \equiv \int d^2x_\perp\, e^{i l_T \cdot x_\perp} \big\langle U(0) U^\dagger(x_\perp) \big\rangle_\rho, \quad (4)$$

with the averaged factor representing the average over all configurations of the color fields sources in the nucleus, $U(x_\perp)$ is a matrix in the $SU(N)$ fundamental representation which represents the interactions of the quark with the classical color field of the nucleus. All the information about the nature of the medium crossed by the quark is included in the function $C(l_T, x_2, A)$. In particular, it determines the dependence on the saturation scale Q_s (and on energy), implying that all saturation effects are encoded in this function. In Ref. [8] we have shown that the saturation effects appear in the function $C(l_T, x_2, A)$ only at small l_T, and as discussed here, the function $\mathcal{W}(p_T, l_T, x_1)$ selects values of l_T larger than p_T, implying that only dileptons with p_T smaller than Q_s should carry information about the CGC. Regarding the structure function $F_2(x_1/z, M^2)$, the CTEQ6L parametrization [19] was used and the lepton pair mass gives the scale for the projectile quark distribution.

The energy dependence introduced in Eq. (2) in the correlator function $C(l_T, x_2, A)$ is performed by means of the saturation scale $Q_s(x_2, A)$ and provides the investigation of the effect of the quantum evolution in the dilepton production. We employed the GBW parametrization [20] to obtain the x dependence of the saturation scale ($Q_s^2 = (x)(x_0/x)^\lambda$), and the parameters have been taken from the dipole cross section extracted from the fit procedure by CGC fit [21] parametrization. The nuclear radius, which appears in Eq. (2), is taken from the parametrization which has the form, $R_A = 1.2A^{1/3}$ fm, while the proton radius (for pp calculations) is taken from the fit [21] ($R_p = 0.6055$ fm).

The function $C(l_T, x, A)$ should be considered as a fundamental quantity in the CGC formalism, since it carries all the information on high density effects. We have evaluated the cross sections using the function $C(l_T, x, A)$ from the mean-field asymptotic solution for the JIMWLK evolution equation [22], introducing an x dependence through the nuclear saturation scale, which is parametrized in the form $Q_s^2(x, A) = A^{1/3} Q_s^2(x)$. It results in a correlator function which is a nonlocal Gaussian distribution of color sources. These considerations imply for the correlator the following form [12,23]

$$C(l_T, x, A) \equiv \int d^2x_\perp \, e^{i l_T \cdot x_\perp} e^{\chi(x, x_\perp, A)}, \tag{5}$$

with

$$\chi(x, x_\perp, A) \equiv -\frac{2}{\gamma c} \int \frac{dp}{p} \big(1 - J_0(x_\perp p)\big) \ln\left(1 + \left(\frac{Q_2^2(x, A)}{p^2}\right)^\gamma\right), \tag{6}$$

where γ is the anomalous dimension ($\gamma \approx 0.64$ for BFKL) and $c \approx 4.84$ [12,23].

One has specified the cross section to evaluate the dilepton differential cross section, and in the next section, the nuclear modification ratio for the dilepton production is investigated and related to the measured Cronin effect.

3. Cronin effect and the dilepton production

As discussed in the introduction of this work, the Cronin effect is present in the measurement of the hadron transverse momentum spectra. Here, the onset of the same effects in the dilepton p_T and rapidity spectra is investigated for a lepton pair mass $M = 6$ GeV. In a previous work [8], the investigation was performed for the p_T distribution of dileptons with mass $M = 3$ GeV. Now, one evaluates the p_T and rapidity spectra for the dilepton at RHIC and LHC energies, $\sqrt{s} = 200$ GeV and $\sqrt{s} = 8800$ GeV, respectively.

We have defined the nuclear modification ratio for the dilepton production in the following form,

$$R_{pA} = \frac{\frac{d\sigma(pA)}{\pi R_A^2 \, dM \, dy \, dp_T^2}}{A^{1/3} \frac{d\sigma(pp)}{\pi R_p^2 \, dM \, dy \, dp_T^2}}. \tag{7}$$

Some attention should be given to the uncertainty in the determination of the nuclear radius, then each cross section is divided by the nuclear or proton radius. The factor $A^{1/3}$ was used in the denominator to guarantee a ratio R_{pA} about 1 at large p_T.

The comparison between the results for the ratio R_{pA} considering two distinct lepton pair masses can be verified in Fig. 1 for LHC energies, where the expected result is found; the effect of the suppression of the ratio is reduced if the dilepton mass is increased at a fixed rapidity. Such result can be verified in Ref. [24], where an analysis was performed for the dilepton production at RHIC and LHC energies in the color-dipole formalism, however, there the ratio was defined with a different normalization.

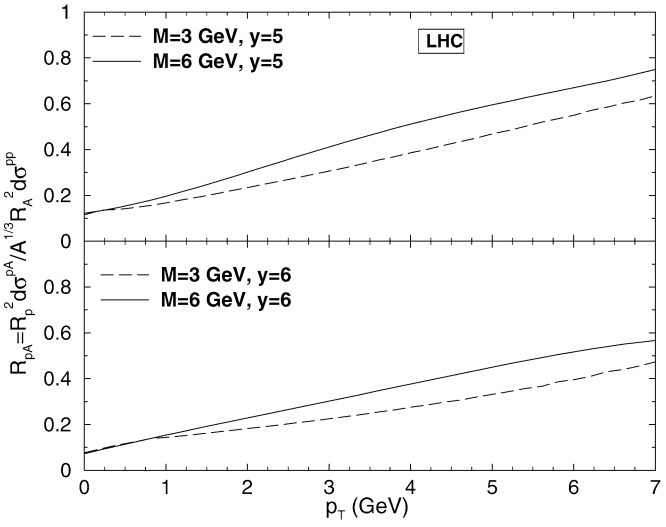

Fig. 1. Ratio R_{pA} for LHC energies, for $y = 5$ and $y = 6$, comparing results for $M = 3$ GeV and $M = 6$ GeV.

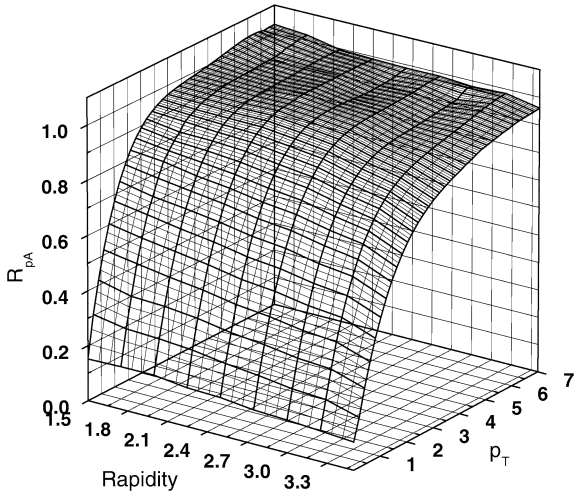

Fig. 2. Ratio R_{pA} as a function of rapidity and p_T for dileptons at RHIC energies.

This analysis regards forward rapidities, which maximum value depends on the value of the mass and the transverse momentum. The region of large mass and large p_T implies smallest values for the rapidity limit. At RHIC energies the maximum rapidity value reaches 4 and at LHC energies it goes up to 7.

In Fig. 2 the nuclear modification ratio for RHIC energies is shown for dilepton mass $M = 6$ GeV. A weak dependence of the ratio R_{pA} with the rapidity range is verified, since for a fixed p_T value, the ratio does not vary significantly with rapidity. This occurs due to the fact that one evaluates the ratio R_{pA} only at forward rapidities, in a short limited range. For the hadron spectra, the suppression of the ratio with the increase of the rapidity is verified for a large range of rapidities, from $y = 0$ to forward ones ($y = 3.2$) [2]. In the case of the dileptons, the same suppression should be verified, however the calculation is restricted to the forward rapidities, providing a small suppression in the rapidity range investigated here. The suppression of

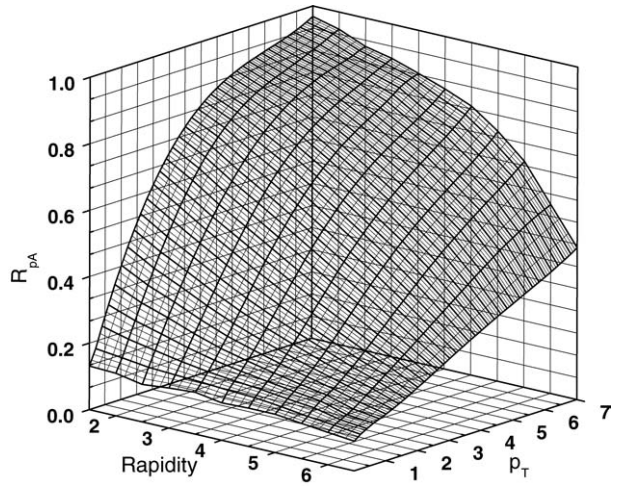

Fig. 3. Ratio R_{pA} as a function of rapidity and p_T for dileptons at LHC energies.

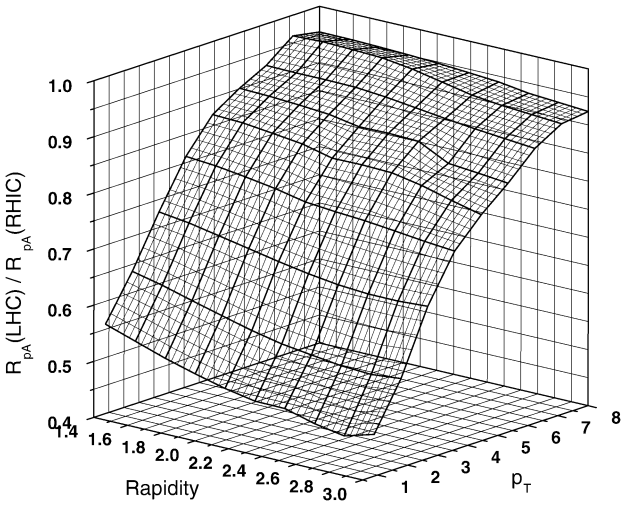

Fig. 4. Ratio between LHC and RHIC ratio R_{pA}.

the ratio (absence of a Cronin type peak) in the p_T distribution is verified, although independent of the rapidity.

In Fig. 3 the nuclear modification ratio for LHC energies is shown for dilepton mass $M = 6$ GeV. Due to the large range of forward rapidities at LHC energies, one verifies the large suppression of the nuclear modification ratio with the increase of the rapidity. This suppression is intensified at large p_T. The suppression of the same ratio with the transverse momentum is also verified and is intensified at large rapidities.

At LHC, the large range of rapidity provides the x range in the large p_T region ($p_T \approx 10$ GeV) between 10^{-4} and 10^{-6}. In this kinematical region, there are significant effects of saturation predicted by the color glass condensate: the large suppression of the nuclear modification ratio comparing with the expected Cronin peak shows the existence of the saturation effects, in both, rapidity and transverse momentum distributions.

The predicted ratio for RHIC and LHC energies is evaluated considering the same description for both, nucleus and nucleons. This implies that the nucleon is not well described, since at intermediated p_T the nucleon is in the linear regime, and we are using a nonlinear approach to the proton. This simplification provides some uncertainty in the ratio at large p_T, mainly at RHIC energies, where the proton saturation scale reaches small values. At LHC energies, the uncertainty in the ratio at large p_T is reduced, since the saturation scale of the proton reaches larger values. The effect of considering a realistic proton appears as a small reduction of the ratio R_{pA} at large p_T, since there is no large suppression in proton gluon density in the linear regime. However, a realistic description of the proton requires the determination of a new parametrization, which is out of the scope of this work.

The comparison between the LHC and RHIC results can be done by means of the ratio $R_{pA}(\text{LHC})/R_{pA}(\text{RHIC})$. This ratio is presented in Fig. 4 which shows that the effect of the suppression is enlarged at LHC, since it presents a severe reduction at small p_T. We are restricted to the RHIC rapidity range to provide this ratio, implying no strong suppression in the rapidity spectra for the ratio $R_{pA}(\text{LHC})/R_{pA}(\text{RHIC})$. The advantage in analyzing such ratio is that it is less sensible to the proton description at large p_T, emphasizing the CGC aspects we meant to explore in this work.

In this work the ratio R_{pA} was investigated in the framework of the CGC for dilepton mass $M = 6$ GeV and shown as a function of rapidity and p_T, demonstrating the effect of suppression in both distributions, rapidity and transverse momentum only at LHC energies. One expects that such saturation effects are from a similar mechanism as observed in the hadrons transverse momentum and rapidity spectra at forward region. This contributes to clarify the status of the Cronin effect as an initial state effect at forward rapidities. The ratio between LHC and RHIC results shows significant saturation effects at LHC compared with the RHIC ones. These features qualify dileptons as a cleanest probe to the color glass condensate dynamics at forward rapidities.

Acknowledgement

This work is supported by the CNPq, Brazil.

References

[1] BRAHMS Collaboration, R. Debbe, J. Phys. G 30 (2004) S759.
[2] BRAHMS Collaboration, I. Arsene, et al., Phys. Rev. Lett. 93 (2004) 242303.
[3] B.Z. Kopeliovich, J. Nemchik, I.K. Potashnikova, M.B. Johnson, I. Scmidt, hep-ph/0501260.
[4] B.Z. Kopeliovich, private communication.
[5] M.A. Betemps, M.B. Gay Ducati, E.G. de Oliveira, in preparation.
[6] D. Kharzeev, Y.V. Kovchegov, K. Tuchin, Phys. Rev. D 68 (2003) 094013; J. Jalilian-Marian, Y. Nara, R. Venugopalan, Phys. Lett. B 577 (2003) 54.
[7] J.L. Albacete, N. Armesto, A. Kovner, C.A. Salgado, U.A. Wiedemann, Phys. Rev. Lett. 92 (2004) 082001.
[8] M.A. Betemps, M.B. Gay Ducati, Phys. Rev. D 70 (2004) 116005.
[9] J. Jalilian-Marian, Nucl. Phys. A 739 (2004) 319.
[10] R. Baier, A.H. Mueller, D. Schiff, Nucl. Phys. A 741 (2004) 358.
[11] J. Jalilian-Marian, Y.V. Kovchegov, hep-ph/0505052.
[12] J.P. Blaizot, F. Gelis, R. Venugopalan, Nucl. Phys. A 743 (2004) 13.
[13] F. Gelis, J. Jalilian-Marian, Phys. Rev. D 66 (2002) 014021.
[14] L. McLerran, R. Venugopalan, Phys. Rev. D 49 (1994) 2233; L. McLerran, R. Venugopalan, Phys. Rev. D 49 (1994) 3352.

[15] J. Jalilian-Marian, A. Kovner, A. Leonidov, H. Weigert, Nucl. Phys. B 504 (1997) 415;
J. Jalilian-Marian, A. Kovner, A. Leonidov, H. Weigert, Phys. Rev. D 59 (1999) 014014.
[16] E. Iancu, A. Leonidov, L.D. McLerran, Nucl. Phys. A 692 (2001) 583;
E. Iancu, A. Leonidov, L.D. McLerran, Phys. Lett. B 510 (2001) 133.
[17] F. Gelis, J. Jalilian-Marian, Phys. Rev. D 66 (2002) 094014.
[18] F. Gelis, A. Peshier, Nucl. Phys. A 697 (2002) 879.
[19] J. Pumplin, D.R. Stump, J. Huston, H.L. Lai, P. Nadolsky, W.K. Tung, JHEP 0207 (2002) 012.
[20] K. Golec-Biernat, M. Wüsthoff, Phys. Rev. D 59 (1999) 014017;
K. Golec-Biernat, M. Wüsthoff, Phys. Rev. D 60 (1999) 114023;
K. Golec-Biernat, M. Wüsthoff, Eur. Phys. J. C 20 (2001) 313.
[21] E. Iancu, K. Itakura, S. Munier, Phys. Lett. B 590 (2004) 199.
[22] E. Iancu, A. Leonidov, L.D. McLerran, Phys. Lett. B 510 (2001) 133.
[23] E. Iancu, K. Itakura, L. McLerran, Nucl. Phys. A 724 (2003) 181.
[24] B.Z. Kopeliovich, J. Raufeisen, A.V. Tarasov, M.B. Johnson, Phys. Rev. C 67 (2003) 014903.